

Supplement of Atmos. Chem. Phys., 15, 10471–10507, 2015
<http://www.atmos-chem-phys.net/15/10471/2015/>
doi:10.5194/acp-15-10471-2015-supplement
© Author(s) 2015. CC Attribution 3.0 License.



Atmospheric
Chemistry
and Physics
Open Access

The logo for the journal Atmospheric Chemistry and Physics, featuring the letters 'EG' inside a circle with a crosshair.

Supplement of

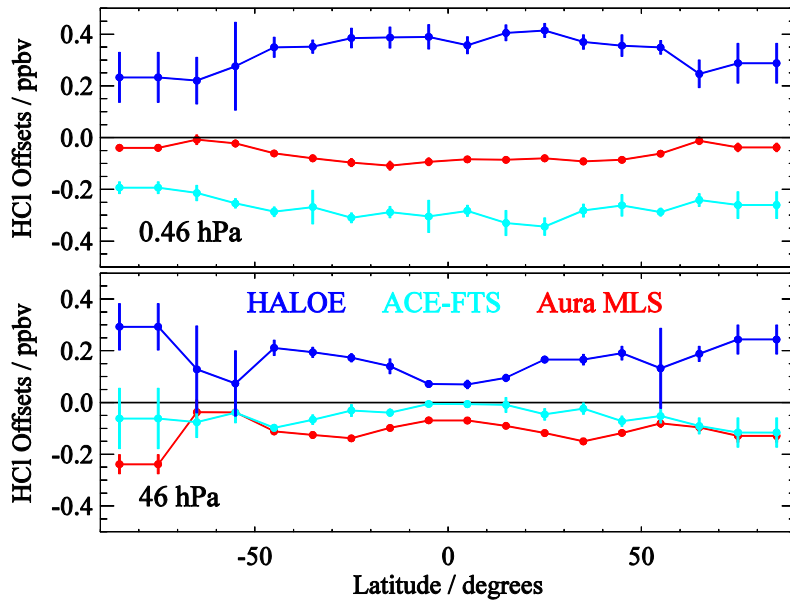
Global OZone Chemistry And Related trace gas Data records for the Stratosphere (GOZCARDS): methodology and sample results with a focus on HCl, H₂O, and O₃

L. Froidevaux et al.

Correspondence to: L. Froidevaux (lucienf@jpl.nasa.gov)

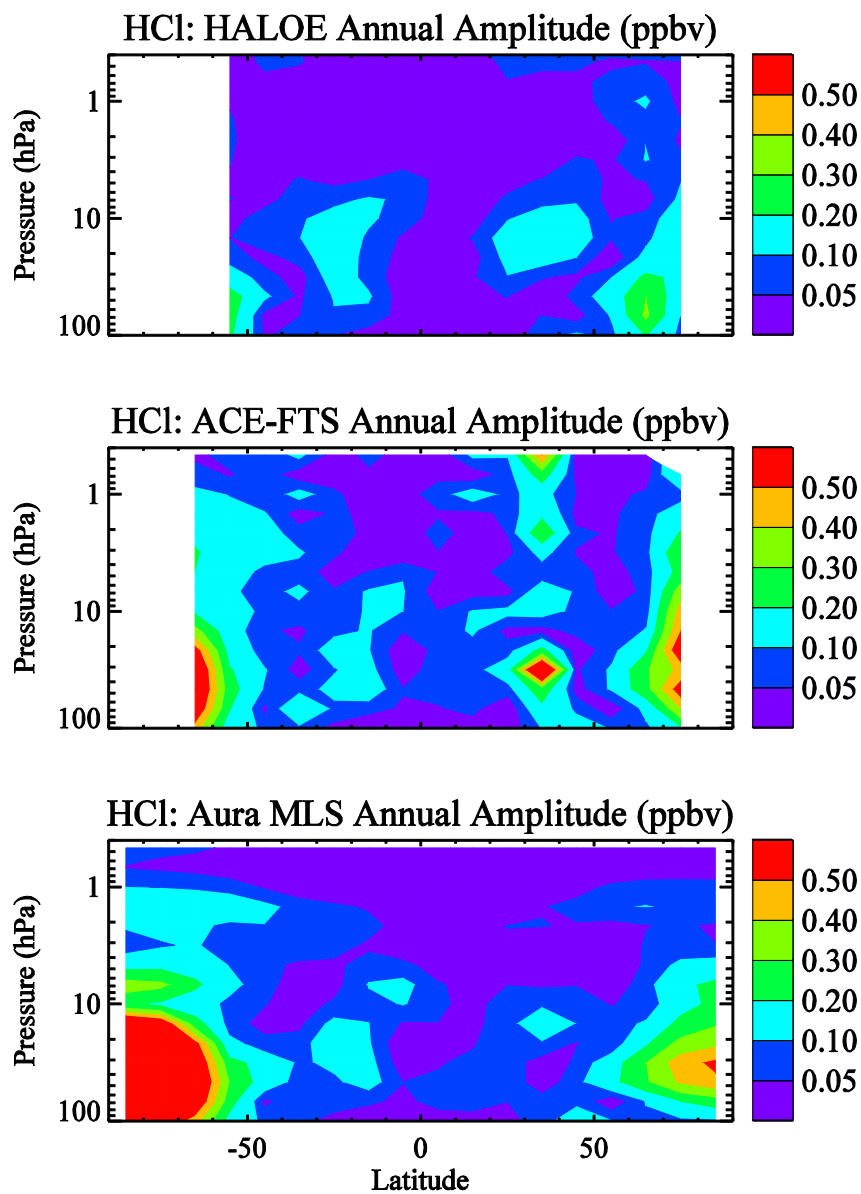
The copyright of individual parts of the supplement might differ from the CC-BY 3.0 licence.

6
7



8
9
10
11
12
13
14
15

Fig. S1: Illustration of the latitudinal dependence of the HCl offsets for HALOE, ACE-FTS, and Aura MLS at two pressure levels (top panel for 0.46 hPa, bottom panel for 46 hPa). Error bars represent twice the standard error in the derived offsets (based on variability during the overlapping period). Larger standard error values indicate that there were either fewer points of overlap or larger offset variability (standard deviations); we found that both of these factors contribute.



16

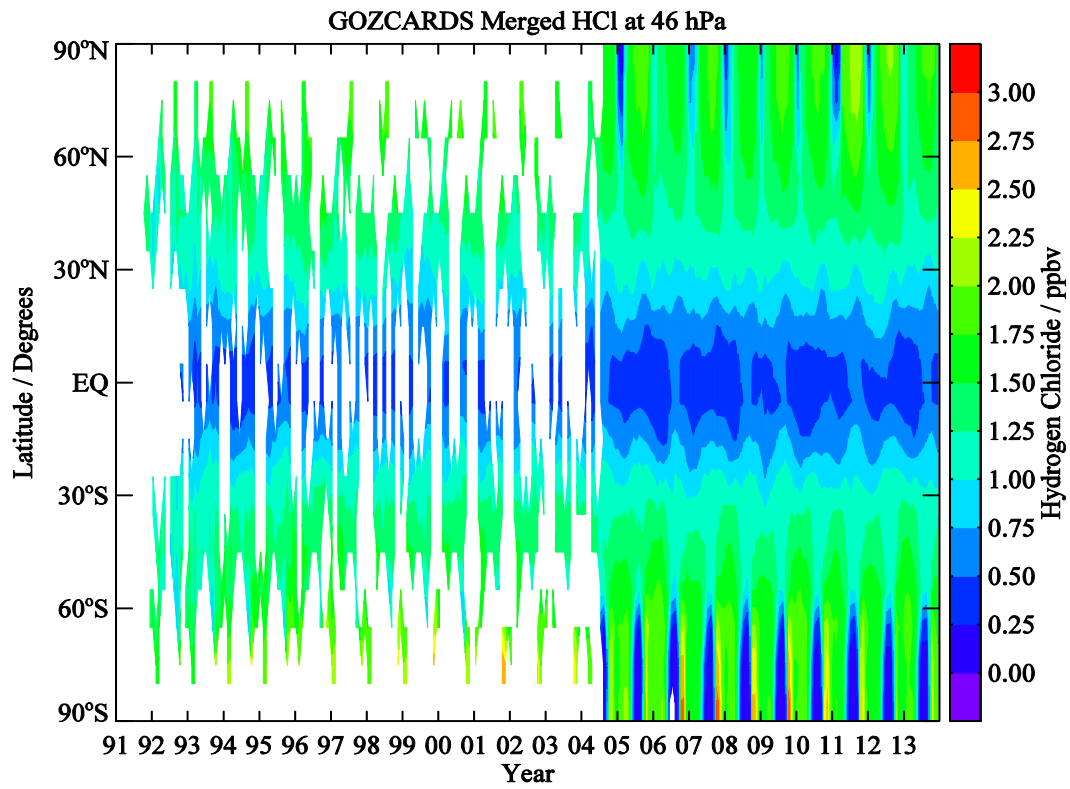
17 **Fig. S2:** Latitude/pressure contours of the fitted mean annual amplitudes (ppbv) from HCl time series for
 18 HALOE, ACE-FTS, and Aura MLS, based on their respective measurement periods (see text).

19

20

21

22

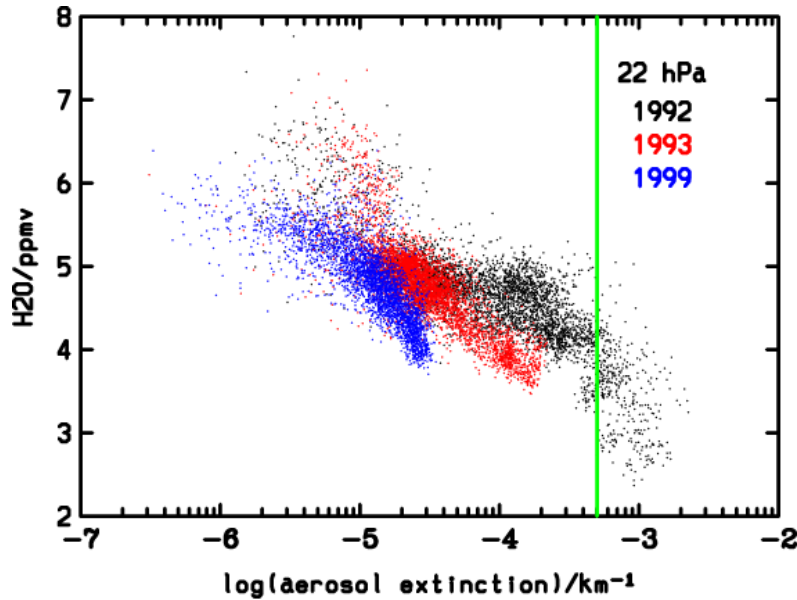


24

25 **Fig. S3:** Time evolution (Oct. 1991 through 2013) versus latitude of GOZCARDS merged HCl (ppbv) at
26 46 hPa.

27

28

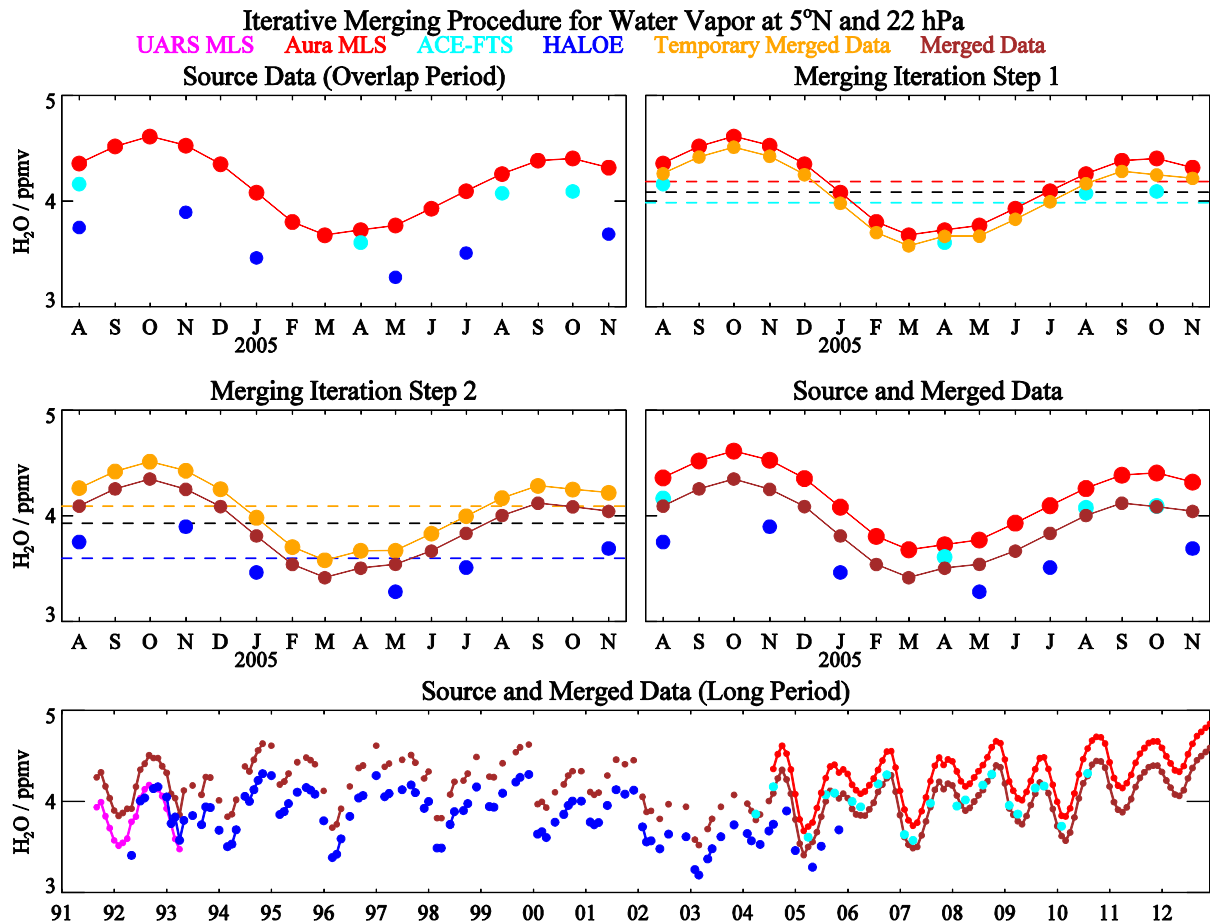


30

31 **Fig. S4:** HALOE sunrise measurements of H₂O versus the 3.46 μm extinction coefficient for 1992, 1993,
32 and 1999 at 22 hPa. The green vertical line represents the aerosol extinction value ($5 \times 10^{-4} \text{ km}^{-1}$) used to
33 screen anomalous HALOE H₂O values. It is apparent that anomalously low H₂O values occurred in 1992
34 when the 3.46 μm aerosol extinction exceeded about $5 \times 10^{-4} \text{ km}^{-1}$. These artifacts were confined to 1991
35 and 1992; for these years, and for pressure levels at and below 22 hPa, the corresponding H₂O data values
36 were excluded. This screening method eliminates about 10% of the global (lower stratospheric)
37 measurements in 1992.

38

39



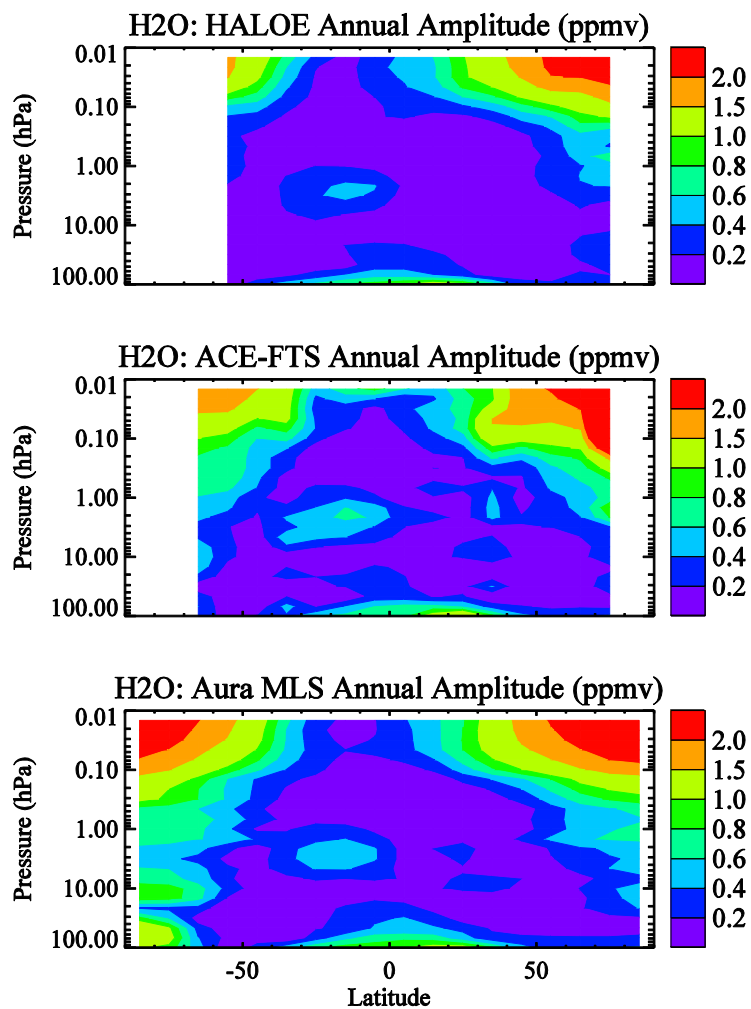
41

42

43 **Fig. S5:** Merging procedure illustration for H_2O at 5°N and 22hPa. This is similar to Fig. 2 (for HCl), but
 44 an additional step is illustrated for the end of this procedure, whereby stratospheric H_2O data from UARS
 45 MLS are adjusted to the early portion of the merged time series that was obtained after the 2nd step; this
 46 adds more coverage (more brown dots in the bottom panel for 1991-1993).

47

48



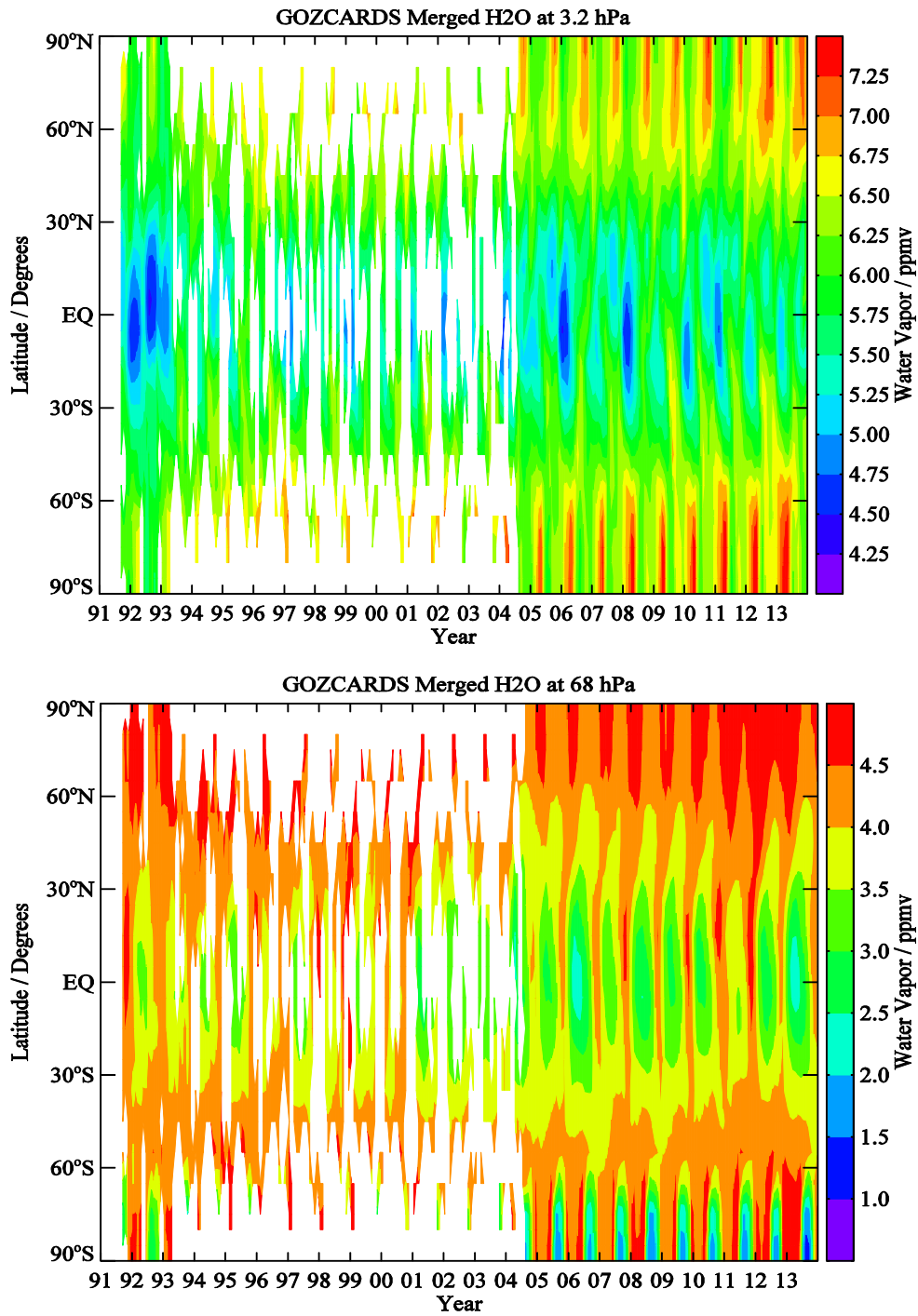
50

51 **Fig. S6:** Latitude/pressure contours of the fitted mean annual amplitudes (ppmv) from H₂O time series for
52 HALOE, ACE-FTS, and Aura MLS, based on their respective measurement periods.

53

54

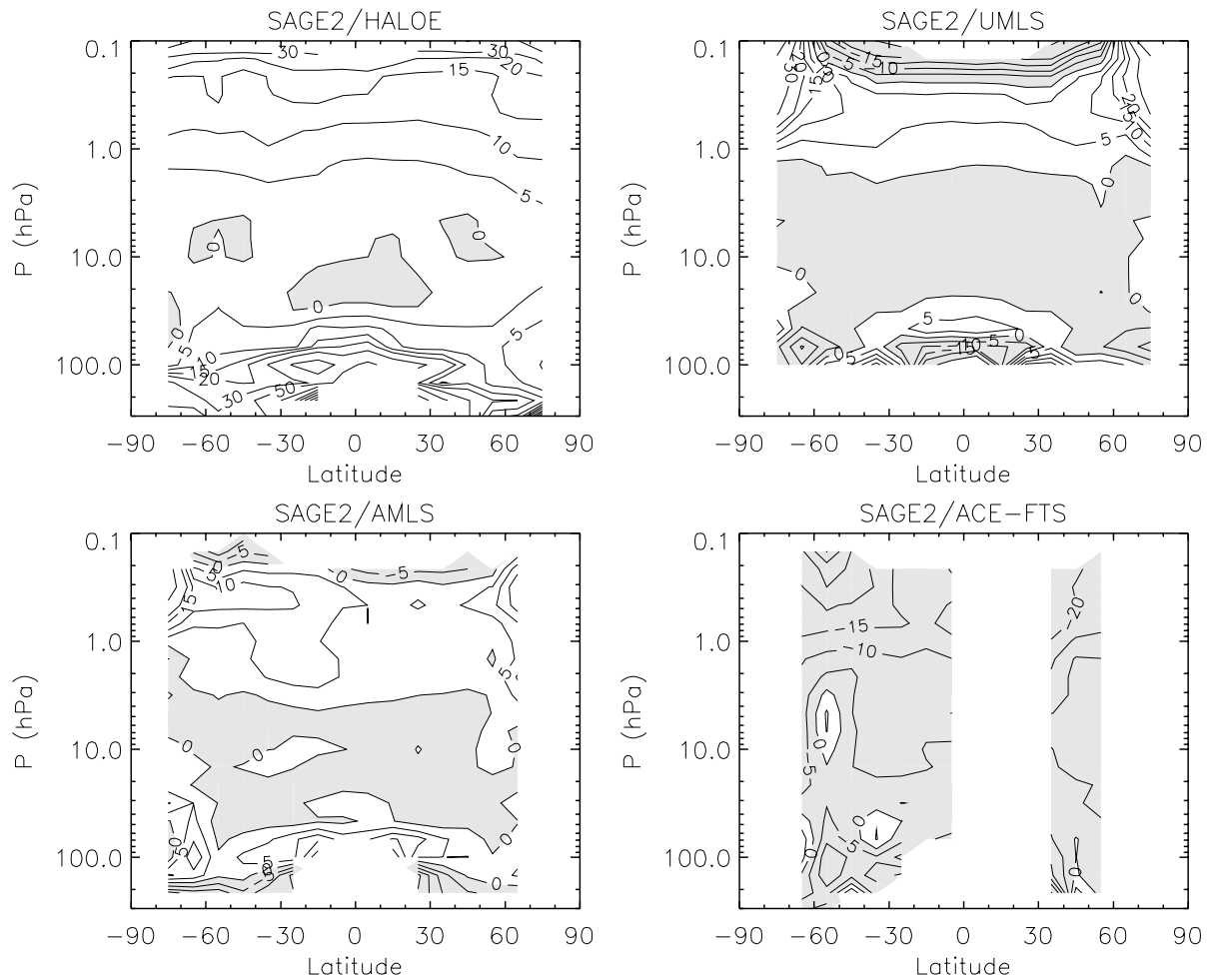
55



56

57 **Fig. S7:** Time evolution (Oct. 1991 through 2013) versus latitude of GOZCARDS merged H₂O (ppmv) at
58 3.2 hPa (top panel) and 68 hPa (bottom panel).

59



61

62 **Fig. S8:** Monthly zonal mean ozone differences (%) between SAGE II and (a) HALOE,
 63 (b) UARS MLS (UMLS for short), (c) Aura MLS (AMLS for short), and (d) ACE-FTS during their
 64 respective overlap periods. Differences are expressed (in percent) as $100 \times [(SAGE\ II - Other) / (Other)]$.
 65 Shaded areas indicate negative values.

66

67

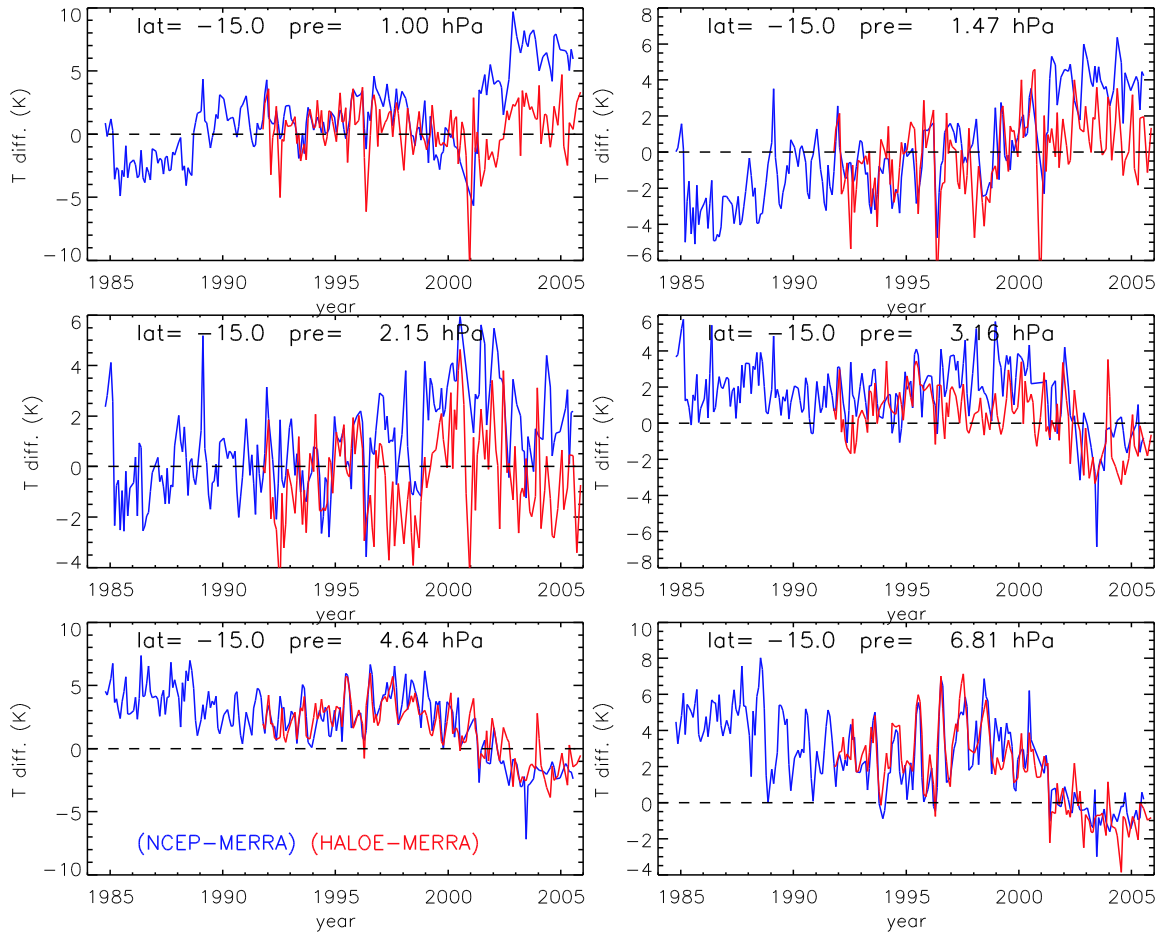
68

69

70

71

72



74

75 **Fig. S9:** Monthly zonal mean temperature differences between NCEP (used by SAGE II) and HALOE
 76 temperatures relative to MERRA for 10°S - 20°S between 1 and 6.8 hPa, per color-coding indicated in
 77 bottom left panel; “pre” represents the pressure value. From 1 to 2.1 hPa, differences between NCEP and
 78 MERRA are generally within ± 4 K before mid-2000. After that time, NCEP temperatures show a sharp
 79 increase and are systematically higher than MERRA values by 5 to 10K. However, this divergence and
 80 trend are not seen in HALOE temperatures. NCEP temperatures between 3.2 and 6.8 hPa are smaller than
 81 MERRA after mid-2000; negative trends (versus MERRA) also occur in the HALOE data at these levels.

82

83

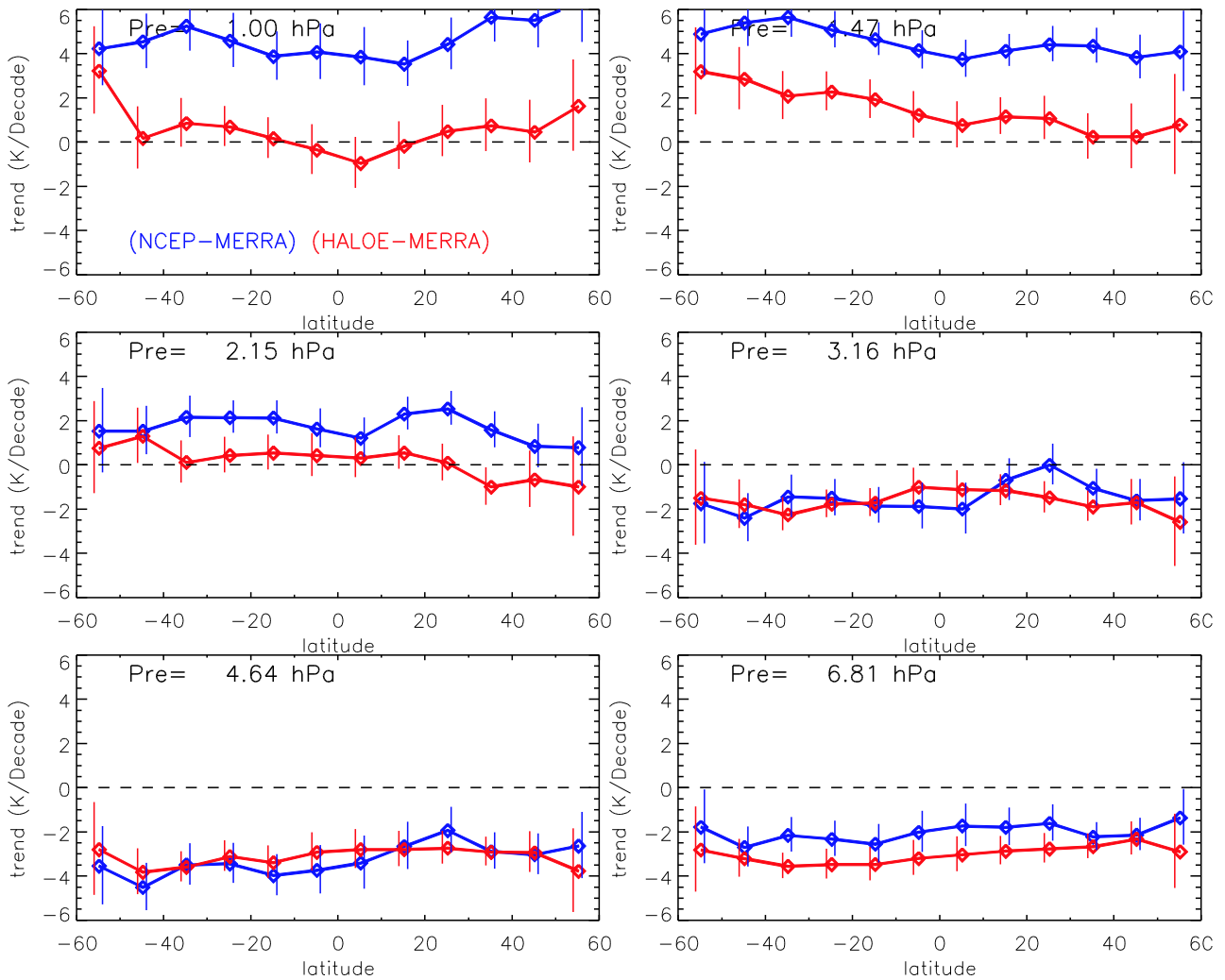
84

85

86

87

88



89

90 **Fig. S10:** Relative trends (K/decade) in zonal mean temperature differences for NCEP – MERRA and
91 HALOE – MERRA (color-coded as in Fig. S9) in the upper stratosphere. NCEP temperatures show
92 positive trends versus MERRA of ~2-5 K/decade between 2.1 and 1 hPa for all latitudes. However,
93 HALOE temperatures show no significant trends versus MERRA, except at 1.5 hPa in the southern
94 hemisphere. For pressures between 3.2 and 6.8 hPa, the temperature analyses are not conclusive; although
95 NCEP values show negative trends of ~2-3 K/decade versus MERRA, they agree with HALOE.

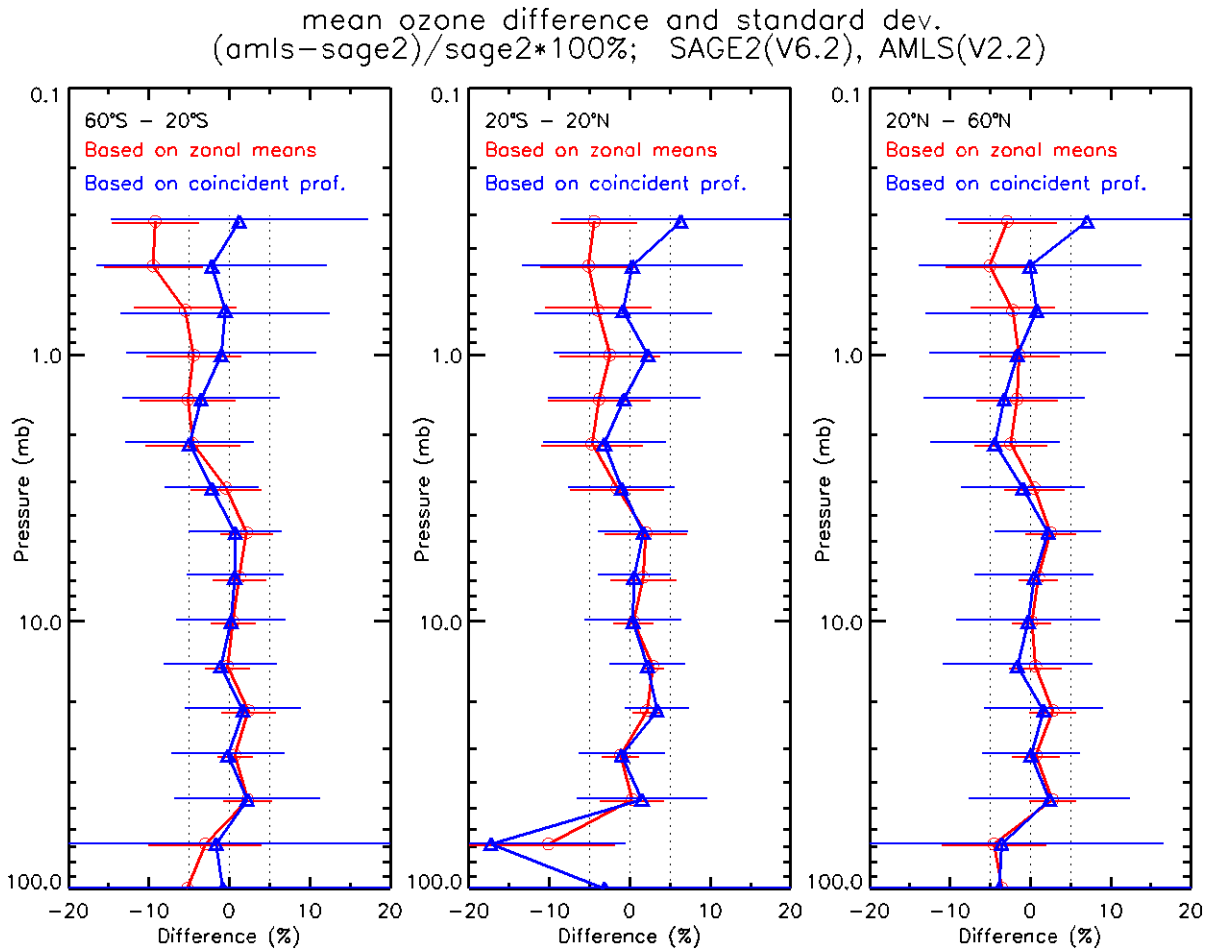
96

97

98

99

100



101

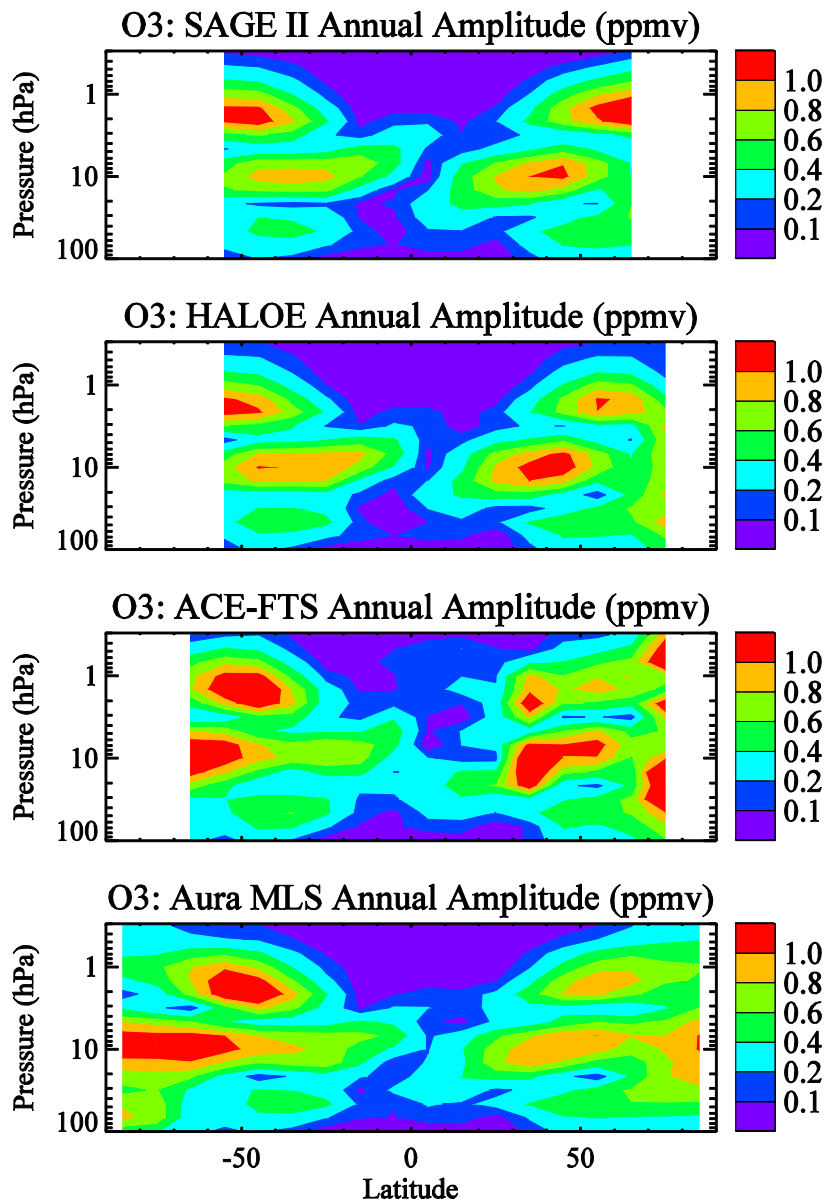
102

103 **Fig. S11:** Mean differences and standard deviations (horizontal bars) between SAGE II and Aura MLS
104 ozone in three different latitude bins: 20°S to 60°S (left panel), 20°S to 20°N (middle panel), and
105 60°N (right panel). Results based on monthly zonal mean and coincident profiles (see text for coincidence
106 criteria) during overlap periods are shown in red and blue, respectively. To choose collocated profiles,
107 coincidence criteria of $\pm 1^\circ$ in latitude and $\pm 8^\circ$ in longitude were used; the time difference criterion was
108 chosen as 12 hours, but only nighttime measurements from Aura MLS were used.

109

110

111



113

114 **Fig. S12:** Latitude/pressure contours of the fitted mean annual amplitudes (ppmv) from O₃ time series for
115 SAGE II, HALOE, ACE-FTS, and Aura MLS, based on their respective measurement periods.

116

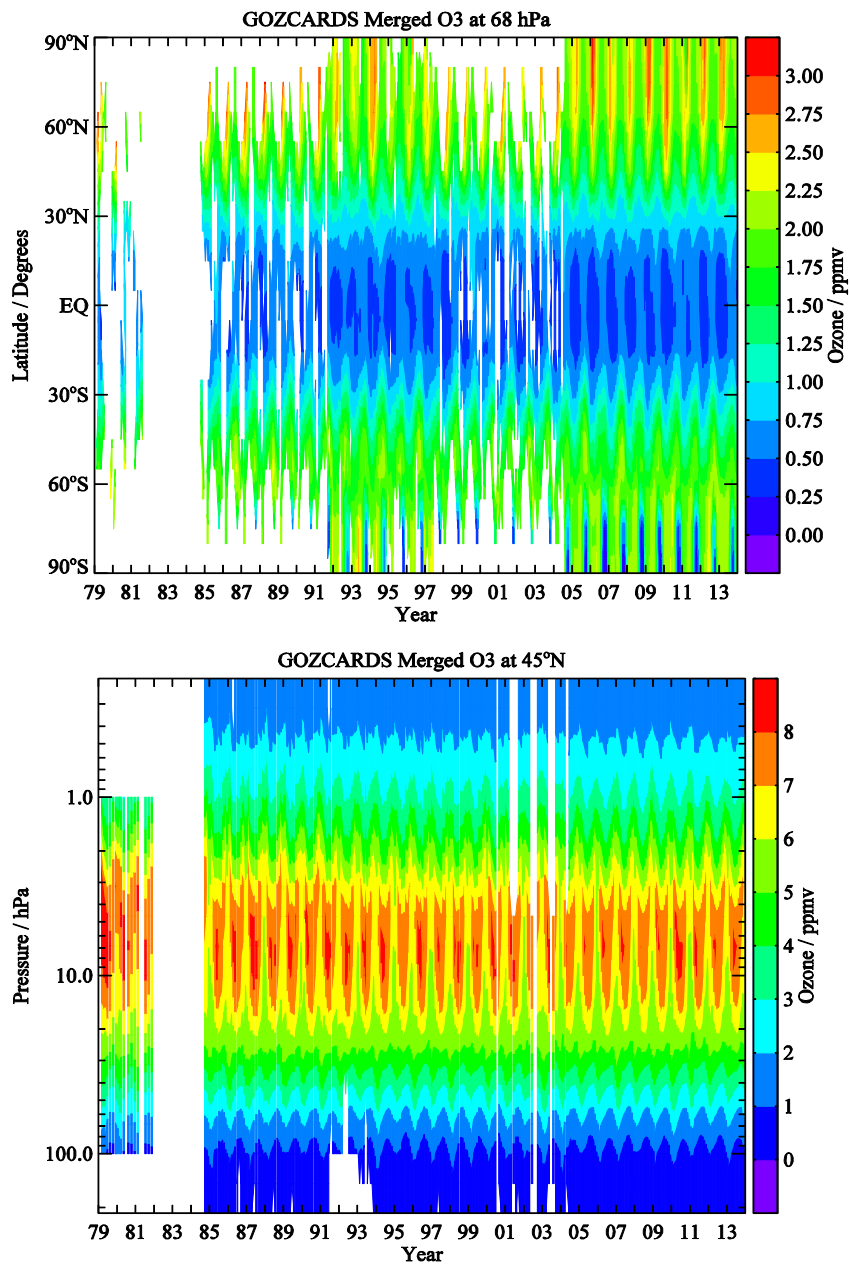
117

118

119

120

121

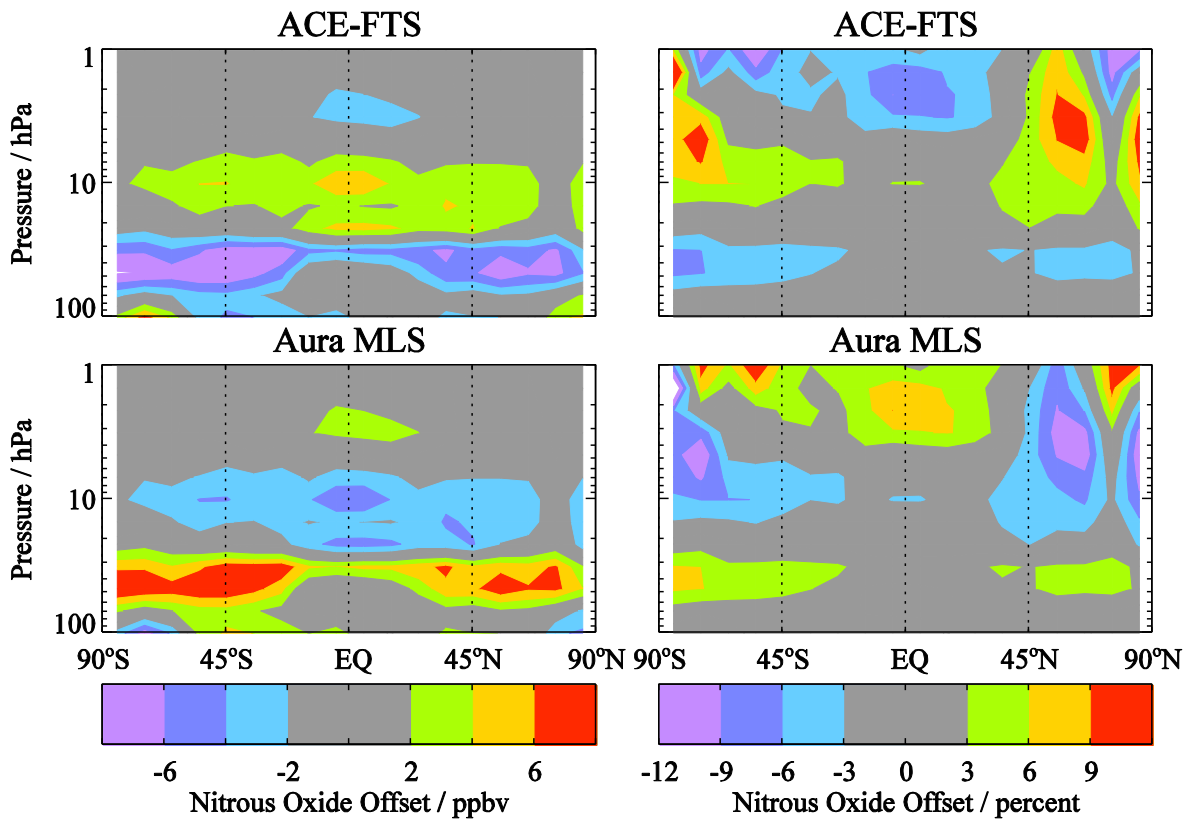


122

123 **Fig. S13:** Illustration of the time evolution of the GOZCARDS merged O₃ data field versus latitude at

124 68 hPa (top panel) and versus pressure for the 40°N-50°N latitude bin (bottom panel).

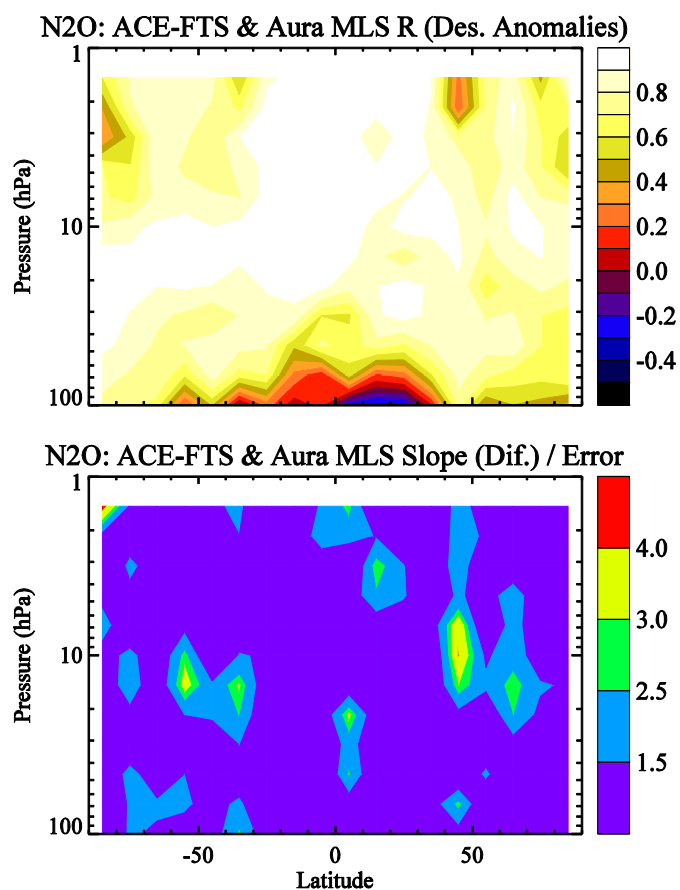
125



126

127 **Fig. S14:** Offsets applied to the N₂O source datasets (top panels for ACE-FTS, bottom panels for Aura
 128 MLS) as a function of latitude and pressure. The left column gives offsets in ppbv and the right column
 129 provides offsets as a percent of the zonal average merged mixing ratios during the overlap period (Aug.
 130 2004 – Sep. 2010) used here to compute the average offsets.

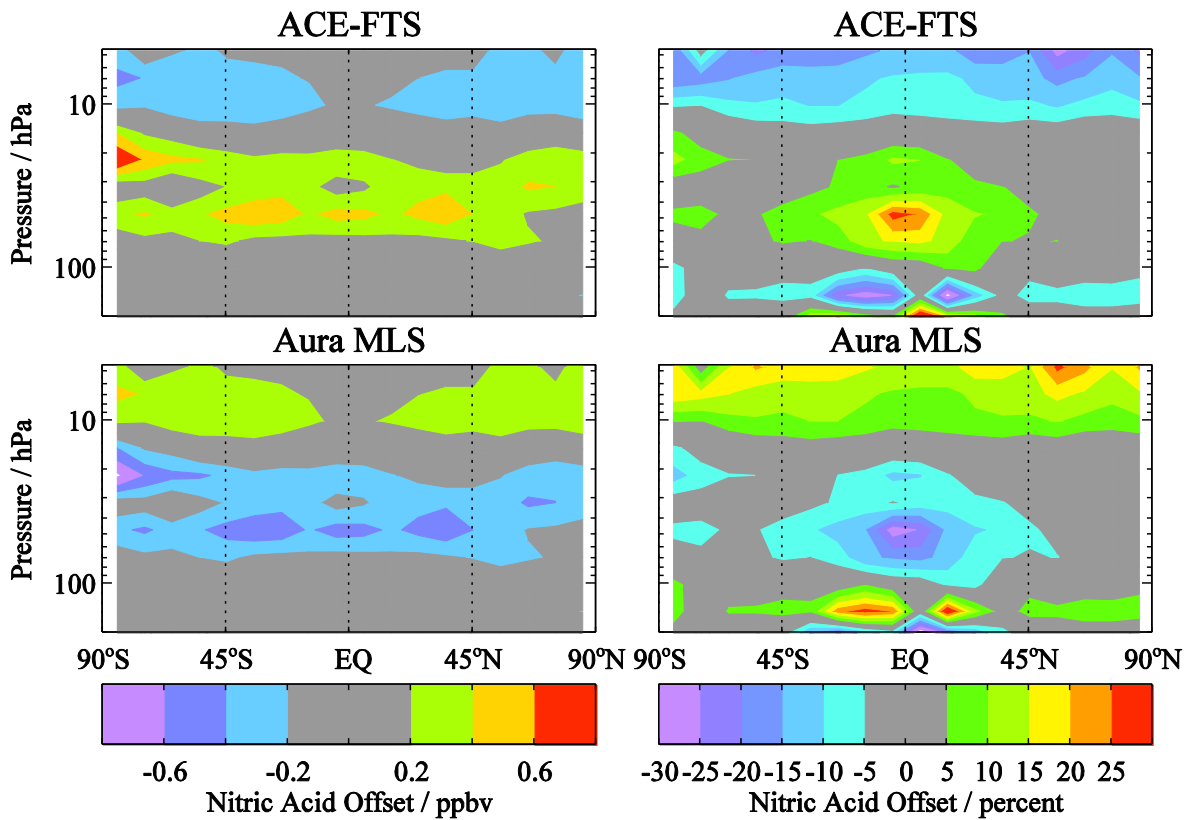
131



132

133 **Fig. S15:** Latitude/pressure contours of time series diagnostics derived from Aura MLS and ACE-FTS
 134 N₂O data comparisons (and obtained from analyses similar to those illustrated in Fig. 6 for HCl). Top
 135 panel: Correlation coefficient for the deseasonalized time series. Bottom panel: Ratio of the slope of the
 136 difference between deseasonalized series over the error in this slope.

137



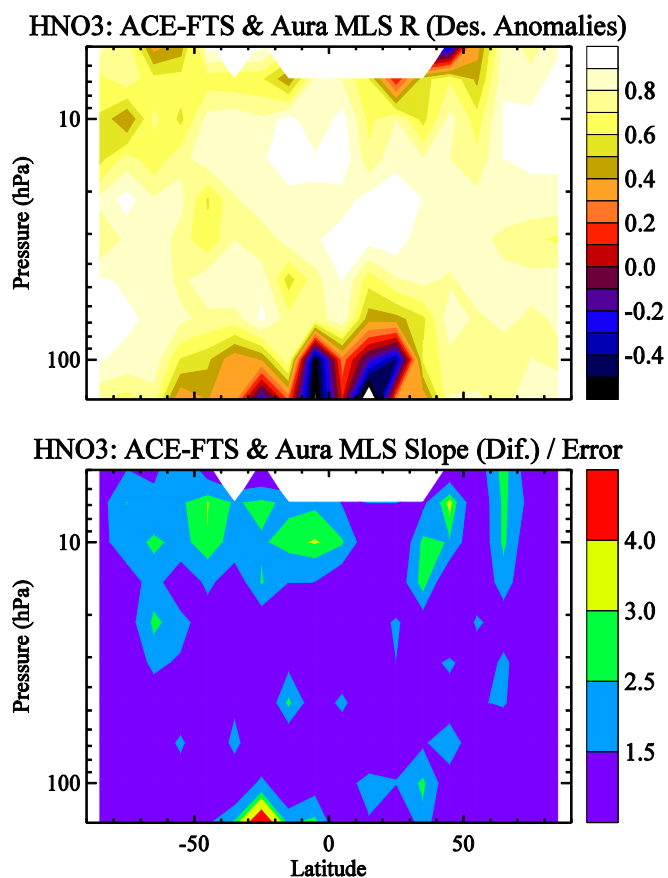
138

139 **Fig. S16:** Offsets applied to the HNO₃ source datasets (top panels for ACE-FTS, bottom panels for Aura
 140 MLS) as a function of latitude and pressure. The left column gives offsets in ppbv and the right column
 141 provides offsets as a percent of the zonal average merged mixing ratios during the overlap period (Aug.
 142 2004 – Sep. 2010) used here to compute the average offsets.

143

144

145



146

147 **Fig. S17:** Latitude/pressure contours of time series diagnostics derived from Aura MLS and ACE-FTS
 148 HNO₃ data comparisons (and obtained from analyses similar to those illustrated in Fig. 6 for HCl). Top
 149 panel: Correlation coefficient for the deseasonalized time series. Bottom panel: Ratio of the slope of the
 150 difference between deseasonalized series over the error in this slope.

151